ACS APPLIED MATERIALS & INTERFACES

Research Article

www.acsami.org

A Scalable Graphene Sulfur Composite Synthesis for Rechargeable Lithium Batteries with Good Capacity and Excellent Columbic Efficiency

Xianfeng Gao, Jianyang Li, Dongsheng Guan, and Chris Yuan*

Department of Mechanical Engineering, University of Wisconsin, Milwaukee, Wisconsin 53201, United States

ABSTRACT: Sulfur nanoparticles wrapped with a conductive graphene framework was synthesized with a high sulfur loading through a scalable one-step process. The graphene-coated sulfur nanostructured composite, when used as cathode for lithium sulfur battery, shows a reversible capacity of 808 mAh g^{-1} at a rate of 210 mA g^{-1} and an average columbic efficiency of ~98.3% over 100 cycles. It is found that graphene oxide (GO) with a porous structure offers flexible confinement function that helps prevent the loss of active materials, thus extending the cycling life of the electrode. Moreover, reduced graphene oxide provides a conductive network surrounding the sulfur particles, which facilitates both electron transport and ion transportation. This novel one-step, all-solution-based process is scalable and provides a promising approach for potential industrial applications.

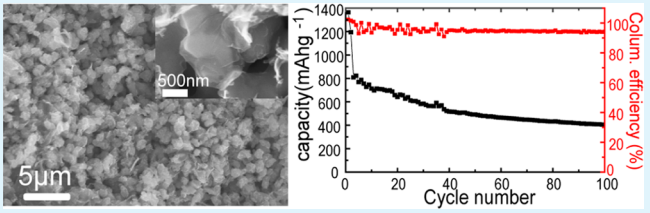

KEYWORDS: *scalable synthesis, graphene-sulfur composite, Li−S battery, high columbic efficiency, energy storage*

1. INTRODUCTION

Elemental sulfur is a promising cathode material for lithium batteries because of its superior intercalation performance. Among all available cathode materials, sulfur possesses a high capacity at 1675 mAh g^{-1} and almost the highest theoretical specific energy at 2600 Wh kg^{-1} if assuming a complete reaction of Li with S in forming Li_2S. However, there are various issues in real practice that prevent sulfur from reaching its theoretical cycling performance during lithium battery charging and discharging.[1−4] The primary issue is that sulfur is both ionically and electrically insulating, which limits the utilization of active materials in lithium batteries.[5] Furthermore, the low-order lithium polysulfide discharge product, such as Li_2S and Li_2S_2, are also expected to be electronic insulators. The second issue is the dissolution of the polysulfide into the electrolyte during the charging and discharging processes.[3,5,6] Without kinetic and chemical constraint, the polysulfide diffuses away from the cathode and crosses over to the Li anode where they are reduced to solid precipitates (Li_2S_2 or Li_2S). Upon charging, these solid precipitates are partially transformed into the polysulfide anions which are then redeposited on the cathode. It is this "shuttle effect" that results in self-discharge and poor columbic efficiency.[7,8]

Various strategies have been employed to alleviate these problems, including employment of electrode coating,[9−11] using conductive additives and multifunctional binders,[12] as well as optimizing organic electrolyte compositions.[13] Nevertheless, the most adoptable method is to disperse sulfur into a conductive and strong adsorbent additive. In this point, various carbonaceous materials, including mesoporous carbon,[14,15] graphene oxide,[16−19] microporous carbon,[20] and carbon nanotube,[21−23] have attracted much attention because of their high conductivity and good electrochemical stability as a cathode additive. Among these materials, graphene oxide offers unique benefits in sulfur-based battery electrodes because of its porous network and superior electric and electrochemical properties, which can significantly improve the transportation of both electrons and ions with the decreased diffusion pathways and interconnection.

In the past, some studies have been conducted on the synthesis of graphene-sulfur nanoparticle hybrids for use on lithium sulfur batteries. Cui et al prepared sulfur graphene composite through a two-step method, in which the sulfur nanoparticles were synthesized first, and then mixed with mildly oxidized graphene oxide under vigorous magnetic stirring.[16] Chen et al dispersed sulfur nanoparticles on graphene oxide sheet followed by reduction of the graphene oxide using hydrazine to get graphene-encapsulated sulfur.[17] Sandwich-like graphene oxide−sulfur composites were also, as synthesized through a combination of solution processes and post-synthesis heat treatment.[24] Although these sulfur graphene hybrids show promising performance, the synthesis pathways that involve multistep processes with a relative high cost and low synthesis efficiency are complex, and consequently limit their use for high sulfur loading and commercial applications.

In this paper, we report a scalable novel sulfur cathode composed of sulfur nano-particles wrapped in a conductive graphene framework that exhibits a high sulfur loading level using a facile one step synthesis method. Comparing with the previous synthesis methods for making graphene sulfur

Received: December 17, 2013
Accepted: February 20, 2014
Published: February 20, 2014

   dx.doi.org/10.1021/am4057979 | *ACS Appl. Mater. Interfaces* 2014, 6, 4154−4159

composite, this method employs sulfur precursor $Na_2S_2O_3$ with ability for graphene oxide reduction, in which the sulfur particles are in situ coated by the reduced graphene in one step reaction. The synthesis results in a bifunctional conformal graphene coating on the sulfur particle, which prevents the loss of the sulfur particles and also acts as continuous electronic conduction pathways. Using the synthesized graphene wrapped sulfur (GWS) electrode, a reversible capacity of 808 mAh g^{-1} at a rate of 210 mA g^{-1} and an average columbic efficiency of ~98.3% over 100 cycles have been achieved.

2. EXPERIMENTAL SECTION

Preparation of Graphene Oxide Wrapped Sulfur. In a typical synthesis, 100 mL of 80 mM sodium thiosulfate ($Na_2S_2O_3$; Aldrich) aqueous solution was mixed with 100 mL of 0.02 wt % PVP (molecular weight of 55 000; Aldrich) at room temperature. Then, the solution was mixed with 10ml graphene oxide (GO) solution (5 mg mL^{-1} in ethanol) and sonifier for 60 min to get a uniform distribution of the precursor. Finally, a stoichiometric amount of 6 M hydrochloric acid was added to the solution under magnetic stirring on a 90 °C hot plate. The resulting suspension was washed three times under centrifugation with water and acetone. Then it was dried in a vacuum oven at 60 °C.

Coin Cell Fabrication. The obtained materials were mixed with carbon black and polyvinylidene difluoride (PVDF, 1.5 wt % in N-Methyl-2-pyrrolidone solution) with a weight ratio of 7:2:1. The slurry was coated on an aluminum foil and dried at 60 °C for 12 h under vacuum condition. In this test, CR2032 coin cells were assembled to evaluate the electrochemical performance of the GWS composite as the cathode material. A Celgard-2320 membrane composed of 20 μm thick polypropylene (PP)/polyethylene/PP tri-layers served as a separator. The electrolyte was 1.0 M lithium bis-(trifluoromethanesulfonyl)imide (LiTFSI) in a mixed solvent of 1,2-dimethoxyethane and 1,3-dioxolane (DOL) with a volume ratio of 1:1 containing 1 wt % $LiNO_3$. Lithium metal foil was used as the counter electrode.

Characterization. Hitachi S-4800 scanning electron microscopy (SEM) was used to characterize the morphology of the graphene wrapped sulfur composite. The composition of the obtained material was analyzed by energy-dispersive X-ray spectroscopy (EDS) integrated with SEM. Thermogravimetric analysis was performed in a nitrogen atmosphere with a heating rate of 10 °C per min from room temperature to 500°C. Cyclic voltammetry (CV) between 3.0 V and 1.5 V at a scanning rate of 0.1 mV s^{-1} and AC impedance over the frequency range from 100 kHz to 0.1 Hz with the amplitude of 5 mV was measured on VersaSTAT 3F (Princeton Applied Research). The charge−discharge cycles were performed between 1.5 and 3 V with LANHE CT2001A (Land) within the same voltage range.

3. RESULTS AND DISCUSSION

In the experiment, the synthesis of the graphene wrapped sulfur composite started from a solution composed of graphene oxide and sodium thiosulfate ($Na_2S_2O_3$). In the solution, $Na_2S_2O_3$ serves both the sulfur precursor and a reducing agent to reduce graphene oxide.[25,26] Sulfur nanoparticles were formed after appropriate amount of HCl added and in situ enveloped by the reduced graphene oxide. The whole process depends on the in situ reduction of $Na_2S_2O_3$ by HCl acid in the presence of the exfoliated graphene oxide. Because of the strong chemical interactions between sulfur and the functional group and sp^2-hybridized carbon of the reduced graphene oxide,[24] the obtained sulfur and reduced graphene oxide can bind to each other and form a core shell structure simultaneously. In addition, feature C originating from the functional C−O bond on the GO will be weakened significantly when incorporated with sulfur,[25] which means strong chemical interactions between S and the functional group of GO and GO is further partially reduced by sulfur during this process. In this synthesis, the relative amount of GO and sulfur precursor may affect the final structure of the composite. In our case, a relative high ratio of sulfur results in a graphene coated sulfur framework. If the graphene has a much higher concentration than sulfur, the formed sulfur will be probably bound directly on the layered GO, and form a sandwich-like structure.[24] Moreover, PVP in the solution also functions as a capping agent for sulfur particles that prevent the formed S particles from aggregation and limit the sulfur particles to the submicrometer size scale during the synthesis.[27] Meanwhile, the size of the formed sulfur particles may also be controlled by adjusting the concentration of wrapping ligand in the synthesis solution.[27] Finally, the GWS composite was obtained after repeated centrifugation and drying. With this one-step approach, reduction of GO and formation of sulfur nanoparticles in situ enveloped by graphene were achieved simultaneously.

For the graphene-wrapped sulfur composite, a characteristic sulfur XRD (Figure 1a) pattern is measured. In the figure, there

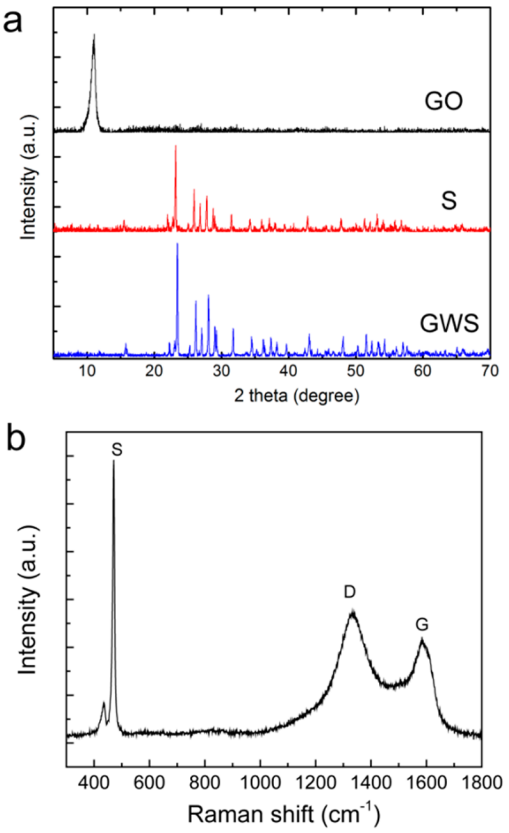

Figure 1. (a) XRD spectra of the graphene oxide (black), sulfur (red), and graphene-wrapped sulfur compound (blue). (b) Raman spectrum of GWS compound with characteristic sulfur peak at~470 cm^{-1}, and the D band (~1350 cm^{-1}) and G band (~1590 cm^{-1}) that are characteristics of graphene.

is no graphite or graphene peaks in the GWS pattern, which indicates that graphene sheets remain in an exfoliated state. No restack process happens during the sulfur particle formation in the synthesis. Raman spectroscopy was performed to further analyzed the sulfur and graphene structure in the GWS composite (Figure 1b). The sulfur particles exhibit a characteristic peak at ~470 cm^{-1}, which is attributed to the characteristic

peak of the symmetric S8 vibrations.[28] The other two prominent peaks at ~1350 and ~1590 cm^{-1} are the D band which represents the dispersive, defect induced vibrations, and the G band which is related to the vibration of sp^2-bonded carbon atoms, respectively. The Raman spectrum indicates that the graphene sheets coated on the sulfur particles in GWS have both disordered and graphitic domains.

SEM images (Figure 2a–c) illustrate the structure of the graphene wrapped sulfur composite under different magnifications. As shown by the figure, sulfur particles were surrounded by the graphene uniformly. The average size of the sulfur particles was found less than 1 μm, which is attributed to the size limiting effect provided by the PVP surfactant coated on the sulfur particles. Moreover, the high magnification SEM image on single sulfur particle (Figure 2c) illustrates the structure of the graphene sulfur composite more clearly, which shows that the inner sulfur particle is well surrounded by the outside graphene layer. The transparency of the graphene sheets reveal that it only consists of a few layers. A strong connection between the sulfur and graphene is obtained, resulting from the in situ coating during the sulfur particle formation process. To verify the structure and composition of the formed compound, energy-dispersive spectroscopic (EDS) line scan was carried out on the obtained material (Figure 2d).

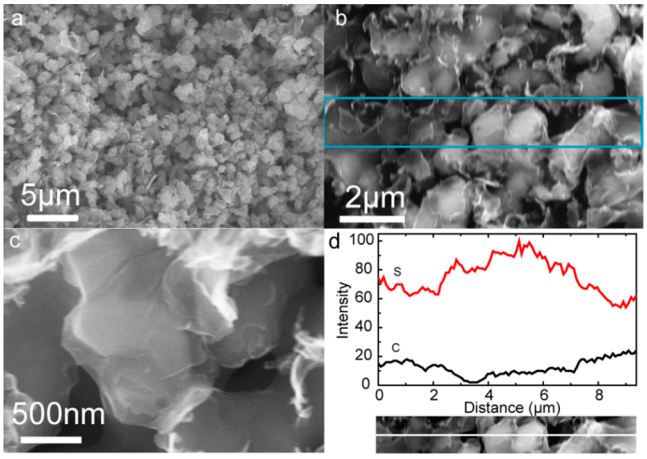

Figure 2. SEM images of graphene-wrapped sulfur compound with (a) low, (b) medium, and (c) high magnifications. (d) EDS line scan spectrum of specific position from image b.

The result confirmed that the bright particles in the SEM images were sulfur particles with carbon coating and interconnected with graphene. Sulfur content was measured with thermogravimetric analysis (Figure 3), giving a mass fraction of 80% in this one-step synthesis. This high mass loading can greatly increase the overall gravimetric capacity of the material with respect to the total mass of cathode.

To identify all the electrochemical reactions in the GWS composite electrode, the cyclic voltammetry (CV) measurement of the GWS composite was conducted at a scan rate of 0.1 mV S^{-1} in the voltage range of 1.5 V to 3 V (Figure 4a). In the cathode scan, two main reduction peaks at around 2.3 and 2.1 V were clearly shown, which result from the multistep reaction mechanisms of sulfur with lithium.[17,20,29] The first step at 2.3 V peak is ascribed to the reduction of elemental sulfur to high-order lithium polysulfides (Li_2S_n, $2 < n < 8$). The second step corresponding to 2.1 V peak can be ascribed to the further reduction of lithium polysulfides to Li_2S_2 or Li_2S. One oxidation

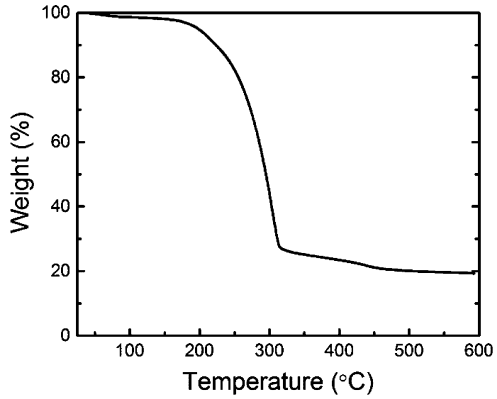

Figure 3. TGA curve (Ar atmosphere) of the graphene-sulfur composite.

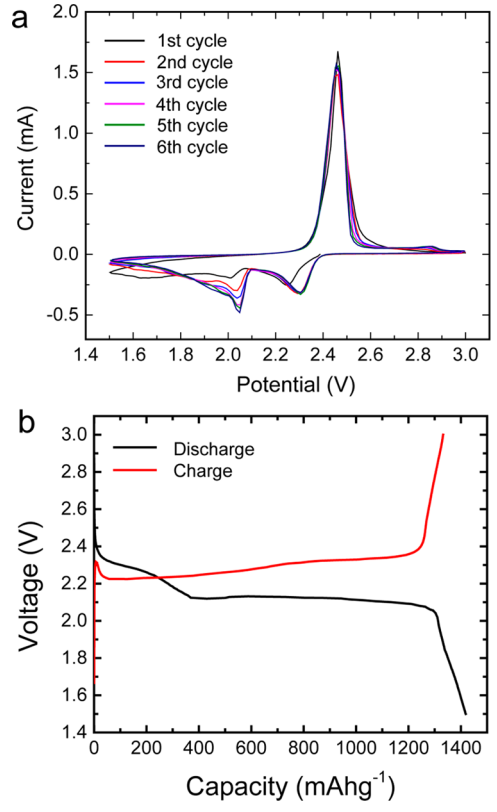

Figure 4. (a) Cyclic voltammograms of the GWS composites at 0.1 mV s^{-1} scanning rate; (b) galvanostatic discharge–charge profiles at current rate of 42 mA g^{-1}.

peak at about 2.4 V can be assigned to the complete conversion of Li_2S and polysulfides into elemental S. In the figure, both cathodic and anodic peaks are positively shifted during the subsequent cycle, attributing to the polarization of the electrode materials in the first cycle. From the 3rd cycle, both the CV peak positions and peak currents showed very small changes, indicating relatively good capacity retention. The CV results show that the GWS composite can help to prevent S from dissolving into the electrolyte and maintain a stable performance. Figure 4b demonstrates the charge-discharge curve of the GWS composite. Two typical plateaus for the S-electrode at 2.3 and 2.1 V are observed in the discharge process, which can be assigned to the two-step reaction of GWS composite in the discharge process. The one plateau observed in the charge

dx.doi.org/10.1021/am4057979 | ACS Appl. Mater. Interfaces 2014, 6, 4154–4159

process at about 2.4 V is resulted from the oxidation process which converts Li_2S and polysulfides to S. The positions of the plateaus correspond well to the typical peaks of the S electrode in the CV curves.

Figure 5a shows the cycling performance and columbic efficiency of the GWS composite cathode at a rate of 210 mA

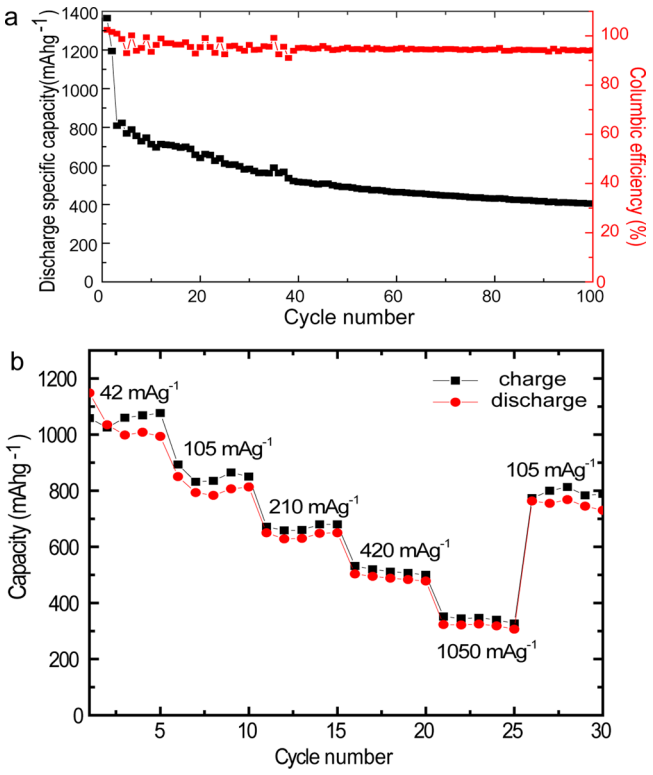

Figure 5. (a) Cycle performance at a constant current rate of 210 mA g^{-1} after initial activation processes at 42 mA g^{-1} for two cycles; (b) rate performance of GWS composite electrode.

g^{-1} after the initial two cycles of activation at 42 mA g^{-1}. An initial discharge capacity of 1364 $mAhg^{-1}$ at a rate of 42 mA g^{-1} is obtained. After the two initial activation processes, the cathode shows a capacity of 808 $mAhg^{-1}$ at a rate of 210 mAg^{-1} and only fade 13.6 % of capacity in the following 15 cycles. The cycling stabilizes after 30 cycles and a very small capacity fade of 6% is observed over the last 20 cycles. A high columbic efficiency of 93.7% is shown even at the 100th cycle (Figure 5a). The average columbic efficiency is obtained as high as 98% during the 100 charge and discharge processes. The initial discharge capacity is comparable with that of the sandwiched GO/sulfur composite[24] and other graphene coated sulfur cathode made with previously reported two steps methods.[16,17] In this structure, the graphene framework contributes to the increasing of conductivity and the acceleration of the ion transfer process. The retention performance could be further improved by reducing the sulfur particle size or optimizing the structure of the composite via adjusting the experimental parameters, which may provide better electron and ion transportation and reduce the active material loss as caused by Li_2S deposition. The remained high columbic efficiency upon cycling confirmed the GWS restrained the shuttle effect successfully. In the obtained GWS composite, the favorable interactions between the lithium polysulfides and reduced graphene oxide play a crucial role in reducing the loss of active mass, which lead to a high columbic efficiency even at 100th cycle. Therefore, it is reasonable to conclude that the capacity loss is not mainly due to the sulfur loss from polysulfide dissolution, which is restrained by the graphene oxide coating. The overall capacity fade is most likely due to the accumulation of insulating Li_2S that are not fully oxidized during the charge process of the cell.

In this study, an excellent rate capability and lower over-discharge are also obtained (Figure 5b). As shown in Figure 5b, with the rapid increase in the charge-discharge current density, the capacity decreased slowly and the over-discharged phenomenon was significantly weakened. At the highest current density of 1050 mA g^{-1}, the measured discharge capacity is 351 mAh g^{-1}. When the current density directly returns to the low value of 105 mA g^{-1} after 25 cycles, the GWS electrode recovers its original capacity, which demonstrates a stable performance of the obtained GWS composite cathode.

Figure 6 shows the Nyquist plots of the battery using the graphene wrapped sulfur composite as a cathode after 1 cycle, 5

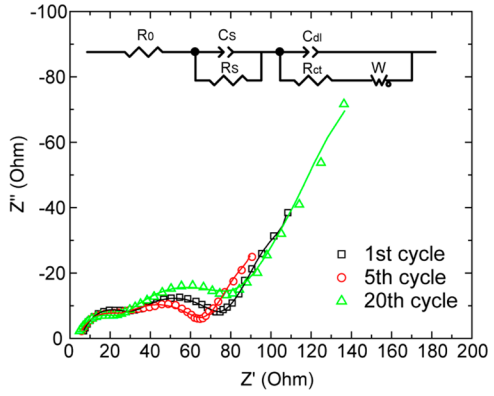

Figure 6. Impedance spectroscopy analysis of GWS composite electrodes cycled for the 1st, 5th, and 20th cycle (the solid lines are fitted plots).

cycles and 20 cycles, with their equivalent circuits. In the figure, all the curves show two semicircles and one linear region, corresponding with particular reaction processes.[30] Specifically, the semicircle at high frequency is considered as the resistance (R_s) and capacitance (C_s) of the accumulated lithium sulfide interface layer formed on the surface of the electrodes. The semicircle in middle frequency region corresponds to charge transfer resistance (R_{ct}) and its relative double-layer capacitance (C_{dl}). R_0 is related to the bulk resistance in the cell and W is the Warburg impedance which corresponds with Li ion diffusion processes in the active material of the electrodes at very low frequencies. The parameters in the model were extracted by fitting the EIS data with ZView software (Table 1). In this model C_S and C_{dl} were both implemented as constant phase elements (CPEs) to compensate for nonideal behavior of rough or porous surface, where C_S-T and C_{dl}-T are related to the values of "pseudo capacitance" of CPEs, whereas C_S-P and C_{dl}-P are corresponding phase parameters. The value of phase parameter demonstrates a parameter of proximity to resistance or capacitance, where 1 performs as a pure capacitor and 0 performs as a pure resistor. Note that the CPE elements vary considerably during the discharge process.[31] The capacitance is not only related with the roughness of the electrode surface and porosity, but also affected by the adsorption/desorption processes involving the electrode and solvent in electrolyte.

dx.doi.org/10.1021/am4057979 | ACS Appl. Mater. Interfaces 2014, 6, 4154−4159

Table 1. Fitted Parameter of Nyquist Plot of GWS Composite Electrodes Cycled for the 1st, 5th, and 20th cycle

	R_0 (Ω)	C_s-T ($\Omega^{-1}cm^{-2}$ s^{-p})	C_s-P	R_s (Ω)	C_{dl}-T ($\Omega^{-1}cm^{-2}s^{-p}$)	C_{dl}-P	R_{ct} (Ω)	W-R (Ω)	W-T (Ω $S^{-1/2}$)	W-P
1st	5.232	2.994×10^{-5}	0.70	22.55	1.282×10^{-3}	0.56	49.27	124.3	64.15	0.57
5th	4.078	3.909×10^{-5}	0.68	17.66	1.415×10^{-3}	0.51	45.71	90.88	84.93	0.54
20th	3.054	6.375×10^{-5}	0.64	19.98	2.023×10^{-3}	0.54	64.92	313.5	136.5	0.58

Therefore, additional information such as the dispersion and surface morphology of the deposited solid product on the electrode, were needed to understand the electrode property by analyzing the capacitance elements. The little fluctuation of the bulk resistance R_0 between 3.054 and 5.232 Ω at different discharge state should contribute to the varied dissolution of the polysulfides at a specific time, which changes the composition as well as the resistance of electrolyte. R_S decreased from 22.55 Ω in the 1st discharge state to 17.66 Ω in the 5th discharge state, reflecting that the relocation of sulfur active materials to the graphene framework reduces the tendency of passivation layer formation on the electrodes upon cycling at the initial stage.[32] After the initial activation process, the device started working under a relatively stable status. The insulating layer grew slowly on the cathode, resulting in a slightly increased R_S of 19.98 Ω in the 20th discharge state. Similarity, the charge transfer resistances R_{ct} calculated from the middle frequency semicircles decreased from 49.27 Ω in the 1st discharge state to 45.71 Ω in the 5th discharge state, as shown in Figure 6. Then the resistance began to increase slowly to 64.92 Ω in the 20th discharge state. The decrease in the charge-transfer resistance is attributed to the activation of the sulfur−Li reaction at discharge−charge cycling. The following little increase of the resistance could be related to the change of the interface charge transfer process in the GWS cathode as induced by the formation and growth of the insulating Li_2S layer. It is worth noting that the results show the charge-transfer resistance of the present coin cell with the GWS composite electrode is much lower and more stable than that of pure sulfur[33] and other graphene-sulfur structure,[18] which demonstrates a charge transfer improvement induced by this core shell structure design with in situ graphene coating. Furthermore, the increase of the resistances of the GWS composite cathode is very little after a relative long cycling test, suggesting an insignificant formation of the Li_2S insulating layer on the surface of the GWS composites, which results in a high columbic efficiency and good cycle performance. In Table 1, Warburg impedance fitting returns three parameters. W-P is the phase parameter of Warburg element. W-R represents the resistance value of Warburg element at very low frequency, which follows the same trend with R_{CT} upon cycling and corresponds with the activation process and the Li_2S insulating layer deposition. W-T represents Warburg coefficient that is related to the diffusion coefficient of the lithium ions in the electrode by the formula $W\text{-}T = L^2/D$, where L is the effective diffusion thickness and D is the diffusion coefficient of the Li ions. The increased W-T values with the cycling reflect a weakened Li ion diffusion upon cycling as induced by the deposited layer on the surface of the electrode, which is an important factor responsible for the battery capacity fading.

4. CONCLUSION

In summary, graphene-wrapped sulfur composite with high sulfur loading was synthesized through a highly scalable approach potential for industry applications. As a result of the uniform distribution of graphene-wrapped sulfur nanoparticles in the composite and conductive graphene network as the electron transportation highway, the composite exhibits a good capacity and remarkable columbic efficiency in the battery testing. The superior performance could be attributed to the unique structures formed through in situ graphene coated sulfur particle synthesis, which results in a bifunctional conformal graphene coating binding to the sulfur particles and serving as continuous effective electronic conduction fortifier. Such a synthetic approach is facile to the synthesis of other composite materials with similar core−shell structure and may be used to help improve the rate capability and cycle performance of the battery in future.

AUTHOR INFORMATION

Corresponding Author

*E-mail: cyuan@uwm.edu. Tel: (414) 229-5639. Fax: (414) 229-6958.

Notes

The authors declare no competing financial interest.

ACKNOWLEDGMENTS

Financial supports from the University of Wisconsin System Applied Research Program and the University of Wisconsin—Milwaukee Bradley and Hertz Catalyst Grant Programs are gratefully acknowledged.

REFERENCES

(1) Bruce, P. G.; Freunberger, S. A.; Hardwick, L. J.; Tarascon, J.-M. Li-O2 and Li-S Batteries with High Energy Storage. *Nat. Mater.* **2012**, *11*, 19−29.

(2) Mikhaylik, Y. V.; Akridge, J. R. Polysulfide Shuttle Study in the Li/S Battery System. *J. Electrochem. Soc.* **2004**, *151*, A1969−A1976.

(3) Ji, X.; Nazar, L. F. Advances in Li-S batteries. *J. Mater. Chem.* **2010**, *20*, 9821−9826.

(4) Barchasz, C.; Leprêtre, J.-C.; Alloin, F.; Patoux, S. New Insights into the Limiting Parameters of the Li/S Rechargeable Cell. *J. Power Sources* **2012**, *199*, 322−330.

(5) Evers, S.; Nazar, L. F. New Approaches for High Energy Density Lithium-Sulfur Battery Cathodes. *Acc. Chem. Res.* **2013**, *46*, 1135−1143.

(6) Manthiram, A.; Fu, Y.; Su, Y. S. Challenges and Prospects of Lithium-Sulfur Batteries. *Acc. Chem. Res.* **2013**, *46*, 1125−1134.

(7) Wang, D.-W.; Zeng, Q.; Zhou, G.; Yin, L.; Li, F.; Cheng, H.-M.; Gentle, I. R.; Lu, G. Q. M. Carbon−Sulfur Composites for Li−S Batteries: Status and Prospects. *J. Mater. Chem. A* **2013**, *1*, 9382−9394.

(8) Cheon, S.-E.; Ko, K.-S.; Cho, J.-H.; Kim, S.-W.; Chin, E.-Y.; Kim, H.-T. Rechargeable Lithium Sulfur Battery. *J. Electrochem. Soc.* **2003**, *150*, A800−A805.

(9) Wu, F.; Chen, J.; Chen, R.; Wu, S.; Li, L.; Chen, S.; Zhao, T. Sulfur/Polythiophene with a Core/Shell Structure: Synthesis and Electrochemical Properties of the Cathode for Rechargeable Lithium Batteries. *J. Phys. Chem. C* **2011**, *115*, 6057−6063.

(10) Lee, J.-H.; Lee, H.-Y.; Oh, S.-M.; Lee, S.-J.; Lee, K.-Y.; Lee, S.-M. Effect of Carbon Coating on Electrochemical Performance of Hard Carbons As Anode Materials for Lithium-Ion Batteries. *J. Power Sources* **2007**, *166*, 250−254.

(11) Lee, K. T.; Black, R.; Yim, T.; Ji, X.; Nazar, L. F. Surface-Initiated Growth of Thin Oxide Coatings for Li−Sulfur Battery Cathodes. *Adv. Energy Mater.* **2012**, *2*, 1490−1496.
(12) Ji, X.; Evers, S.; Black, R.; Nazar, L. F. Stabilizing Lithium-Sulphur Cathodes Using Polysulphide Reservoirs. *Nature communications* **2011**, *2*, 325.
(13) Hassoun, J.; Scrosati, B. Moving to a Solid-State Configuration: A Valid Approach to Making Lithium-Sulfur Batteries Viable for Practical Applications. *Adv. Mater.* **2010**, *22*, 5198−5201.
(14) Liang, C.; Dudney, N. J.; Howe, J. Y. Hierarchically Structured Sulfur/Carbon Nanocomposite Material for High-Energy Lithium Battery. *Chem. Mater.* **2009**, *21*, 4724−4730.
(15) Demir-Cakan, R.; Morcrette, M.; Nouar, F.; Davoisne, C.; Devic, T.; Gonbeau, D.; Dominko, R.; Serre, C.; Férey, G.; Tarascon, J.-M. Cathode Composites for Li−S Batteries via the Use of Oxygenated Porous Architectures. *J. Am. Chem. Soc.* **2011**, *133*, 16154−16160.
(16) Wang, H.; Yang, Y.; Liang, Y.; Robinson, J. T.; Li, Y.; Jackson, A.; Cui, Y.; Dai, H. Graphene-Wrapped Sulfur Particles As a Rechargeable Lithium-Sulfur Battery Cathode Material with High Capacity and Cycling Stability. *Nano Lett.* **2011**, *11*, 2644−2647.
(17) Xu, H.; Deng, Y.; Shi, Z.; Qian, Y.; Meng, Y.; Chen, G. Graphene-Encapsulated Sulfur (GES) Composites with a Core-Shell Structure As Superior Cathode Materials for Lithium-Sulfur Batteries. *J. Mater. Chem. A* **2013**, *1*, 15142−15149.
(18) Wang, J.-Z.; Lu, L.; Choucair, M.; Stride, J. A.; Xu, X.; Liu, H.-K. Sulfur-Graphene Composite for Rechargeable Lithium Batteries. *J. Power Sources* **2011**, *196*, 7030−7034.
(19) Cao, Y.; Li, X.; Aksay, I. A.; Lemmon, J.; Nie, Z.; Yang, Z.; Liu, J. Sandwich-Type Functionalized Graphene Sheet-Sulfur Nanocomposite for Rechargeable Lithium Batteries. *Phys. Chem. Chem. Phys.* **2011**, *13*, 7660−5.
(20) Jayaprakash, N.; Shen, J.; Moganty, S. S.; Corona, A.; Archer, L. A. Porous Hollow Carbon@Sulfur Composites for High-Power Lithium−Sulfur Batteries. *Angew. Chem., Int. Ed.* **2011**, *50*, 5904−5908.
(21) Yuan, L.; Yuan, H.; Qiu, X.; Chen, L.; Zhu, W. Improvement of Cycle Property of Sulfur-Coated Multi-Walled Carbon Nanotubes Composite Cathode for Lithium/Sulfur Batteries. *J. Power Sources* **2009**, *189*, 1141−1146.
(22) Guo, J.; Xu, Y.; Wang, C. Sulfur-Impregnated Disordered Carbon Nanotubes Cathode for Lithium-Sulfur Batteries. *Nano Lett.* **2011**, *11*, 4288−4294.
(23) Zhou, G.; Wang, D.-W.; Li, F.; Hou, P.-X.; Yin, L.; Liu, C.; Lu, G. Q.; Gentle, I. R.; Cheng, H.-M. A Flexible Nanostructured Sulphur−carbon Nanotube Cathode with High Rate Performance for Li-S Batteries. *Energy Environ. Sci.* **2012**, *5*, 8901.
(24) Ji, L.; Rao, M.; Zheng, H.; Zhang, L.; Li, Y.; Duan, W.; Guo, J.; Cairns, E. J.; Zhang, Y. Graphene Oxide as a Sulfur Immobilizer in High Performance Lithium/Sulfur Cells. *J. Am. Chem. Soc.* **2011**, *133*, 18522−18525.
(25) Chen, W.; Yan, L.; Bangal, P. R. Chemical Reduction of Graphene Oxide to Graphene by Sulfur-Containing Compounds. *J. Phys. Chem. C* **2010**, *114*, 19885−19890.
(26) Li, N.; Zheng, M.; Lu, H.; Hu, Z.; Shen, C.; Chang, X.; Ji, G.; Cao, J.; Shi, Y. High-rate lithium-sulfur batteries promoted by reduced graphene oxide coating. *Chem. Commun.* **2012**, *48*, 4106−4108.
(27) Chen, H.; Dong, W.; Ge, J.; Wang, C.; Wu, X.; Lu, W.; Chen, L. Ultrafine Sulfur Nanoparticles in Conducting Polymer Shell as Cathode Materials for High Performance Lithium/Sulfur Batteries. *Sci. Rep.* **2013**, *3*.
(28) Ward, A. T. Raman Spectroscopy of Sulfur, Sulfur-Selenium, And Sulfur-Arsenic Mixtures. *J. Phys. Chem.* **1968**, *72*, 4133−4139.
(29) Peled, E. Lithium-Sulfur Battery: Evaluation of Dioxolane-Based Electrolytes. *J. Electrochem. Soc.* **1989**, *136*, 1621−1625.
(30) Andre, D.; Meiler, M.; Steiner, K.; Wimmer, C.; Soczka-Guth, T.; Sauer, D. U. Characterization of High-Power Lithium-Ion Batteries by Electrochemical Impedance Spectroscopy. I. Experimental Investigation. *J. Power Sources* **2011**, *196*, 5334−5341.
(31) Deng, Z.; Zhang, Z.; Lai, Y.; Liu, J.; Li, J.; Liu, Y. Electrochemical Impedance Spectroscopy Study of a Lithium/Sulfur Battery: Modeling and Analysis of Capacity Fading. *J. Electrochem. Soc.* **2013**, *160*, A553−A558.
(32) Zu, C.; Su, Y. S.; Fu, Y.; Manthiram, A. Improved Lithium-Sulfur Cells with a Treated Carbon Paper Interlayer. *Phys. Chem. Chem. Phys.* **2013**, *15*, 2291−2297.
(33) Yuan, L.; Qiu, X.; Chen, L.; Zhu, W. New Insight into the Discharge Process of Sulfur Cathode by Electrochemical Impedance Spectroscopy. *J. Power Sources* **2009**, *189*, 127−132.